

# **Hamburger Beiträge**

## **zur Angewandten Mathematik**

### **Duality based error estimation in the presence of shocks**

Susanne Beckers, Jörn Behrens, Winnifried Wollner

Nr. 2016-21  
September 2016



## Duality based error estimation in the presence of shocks

Susanne Beckers · Jörn Behrens ·  
Winnifried Wollner

the date of receipt and acceptance should be inserted later

**Abstract** The dual-weighted-residual method for goal-oriented error estimation relies on the evaluation of weighted residuals. In standard weak form of hyperbolic problems all derivatives are moved to the test function as potential discontinuities prohibit (weak) derivatives for the solution. Since the same holds true for the dual problem, multiplication of residuals and weights is not well defined in the situation of coinciding discontinuities.

In this paper, the problem of coinciding discontinuities is alleviated by adding artificial viscosity to the dual equation, while leaving the primal problem unchanged. This procedure introduces an additional residual term in the error estimation, accounting for the inconsistency between primal and dual problem.

The effectivity of the extended error estimator, estimating the global error in the functional of interest, is tested numerically. The extended error estimator and an unmodified estimator perform similarly regarding refinement indicators. However, only the modified method provides an efficient error estimator.

**Keywords** dual weighted residual · hyperbolic problems · discontinuous Galerkin · error estimation

**Mathematics Subject Classification (2010)** 65M15 · 65M60

---

S. Beckers

Dept of Mathematics, Universität Hamburg, Bundesstraße 55, 20146 Hamburg, Germany  
E-mail: susannebeckers@uni-hamburg.de

J. Behrens

Dept of Mathematics, Universität Hamburg, Bundesstraße 55, 20146 Hamburg, Germany

W. Wollner

Dept of Mathematics, Technische Universität Darmstadt, Dolivostr. 15, 64293 Darmstadt, Germany

**Acknowledgements** This research was partially supported by *Forschungs- und Wissenschaftsstiftung Hamburg*. We also like to thank Dr. Stefan Vater from the University of Hamburg/ClISAP for the code he shared, which gave a basis for the 1D dG advection code.

## 1 Introduction

Adaptive grid refinement requires local error indicators. [1], [2], [26], and many others specified residual-based error estimators for the finite element method for a wide variety of partial differential equations. In contrast to the previous error estimates for global error norms, goal-oriented error estimation considers the error estimation for a, post-processed, quantity of interest, see, e.g., [1, 5, 9]. In the goal-oriented context, the dual-weighted-residual (DWR) method, cf., [5], provides an error estimator consisting of weighted residuals of the primal and dual equation. In contrast to elliptic and parabolic problems, the derivation of DWR estimates for hyperbolic problems is complicated by the fact that, in general, the solution to the formal dual problem is not sufficiently regular to be used as a test function for the primal equation, see, e.g., [21]. A standard approach to circumvent this problem, cf., [21], is the consideration of an elliptic regularization/stabilization for the equation considered. While this approach coincides with the standard discretization with continuous finite elements, additional stabilization is not so natural for discontinuous Galerkin methods (dG).

In this paper, we will derive a DWR error representation for dG discretizations of hyperbolic problems that require a stabilization only for the, auxiliary, dual problem while leaving the primal problem unchanged.

Indeed the problem of finding a suitable representation of the error in the quantity of interest via adjoint calculus has to be expected since differentiability of such functionals w.r.t. the problem data is a subtle issue, see for instance [22], [23], and [11], where the problem was tackled by “shift differentiability”, suitably modified adjoint based derivative computations, and application of artificial viscosity to the primal and adjoint equations, respectively.

In this paper, the appearance of discontinuities is only suppressed in the dual solution by modification of the dual equation providing an adjoint based error representation. Due to the modified dual problem, the resulting error representation will contain an additional residual term. It is then shown numerically that this term is needed to obtain an effective error estimate, while it is not necessarily needed for mesh refinement indicators.

The DWR error representation can not be evaluated in general because the weights contain the unknown, primal and dual, solution. Consequently, the weights need to be approximated utilizing the discrete, primal and dual, solutions. The discrete weight approximations can then be used withing the DWR error representation (formal DWR); regardless of whether the exact weight is suitable for this task or not. The difficulties in using the exact weight will consequently give rise to a more subtle matter in the DWR method; namely if the exact weight is not suitable in the representation, then it is

not clear why the approximate weight should give an accurate error estimate. Indeed, we will see numerically that the quality of the error estimate provided by a formal DWR estimator without modified dual will be worse than the one given by our proposed method in the case where the exact weights are not suitable to be inserted into the error identity.

While there are two ways to obtain a discrete adjoint problem; either by discretization of the continuous adjoint equation or by adjoining the discrete primal equation. This plays no role in our argument as the non-existence of the continuous error representation will give equal trouble in both cases. Moreover, in pure Galerkin-discretizations both approaches will coincide. The discrete adjoint is often used, e.g., [16], [15], and [24], due to the simplicity of applying an automatic adjoining algorithm. But also continuous adjoint models were developed: In [4] a continuous adjoint model of the shallow water equations is derived to apply the DWR method with r-adaptivity for a finite element discretization. In [20] the element-wise continuous adjoint model of the Euler equations is applied and discretized by the finite volume method. In both cases the primal and dual solution were sufficiently smooth such that the solutions can be used as weights for the residuals. As mentioned above, this is not the general case as the weighted residuals of the advection equation are not bounded in general, if neither the primal solution nor the dual solution are weakly differentiable in space.

The paper is organized as follows: In Section 2, a motivation is given to consider the property of weak differentiability of the primal or dual solution in connection with the DWR method with continuous adjoints. The next section, Section 3, gives a simple 1D example for the advection equation and its dual as well as the advection diffusion equation and its dual. In all cases the solutions can be computed analytically. However, if both solutions have coinciding discontinuities, the residual of the advection equation can not be tested with the dual solution. In Section 4, the dual equation is modified by adding artificial diffusion, such that even for discontinuous initial conditions the dual solution is smooth and can be used as a weight for the DWR method. The modification of the dual equation results in an additional residual for the error estimation. Section 5 states the precise discretization utilized for our numerical experiments in Section 6. The numerical experiments confirm that the modified adjoint is advantageous compared to the formal DWR method when one estimates the error, and not only uses the indicators for mesh refinement.

## 2 Motivation

For the use of the DWR method, it is suitable to rewrite the conservation law in weak form. In this context, let  $a(\cdot, \cdot): W \times V \rightarrow \mathbb{R}$  be a semi-linear form, i.e., it is linear in its second component, and let  $F(\cdot)$  be a linear functional on  $V$ .

Suppose that  $u \in W$  is a solution of

$$a(u, \psi) = F(\psi) \quad \forall \psi \in V, \quad (1)$$

where  $W$  is a suitable function space and  $V$  is the proper test function space.

The weak form might also be utilized for discretization, such as the finite element or finite volume method. If the discrete solution  $u^{hk}$  on a spatial mesh with element size  $h$  and time step size  $k$  is to be post-processed by evaluating a goal-functional  $J$ , a natural question is the sensitivity of the functional value with respect to, small, perturbations. To this end it is useful to consider the adjoint solution  $z \in V$  of

$$a'(u; \phi, z) = J'(u; \phi), \quad \forall \phi \in W \quad (2)$$

Due to the definition of the primal and adjoint solution  $u \in W$  and  $z \in V$  should hold. For a reasonable problem the primal solution is indeed in  $W$ , but the adjoint problem (2) does not necessarily have a solution in the space  $V$ ! To see that this is in fact a problem, we discuss this along a simple example.

For an advection equation a natural space is  $W = L^\infty(\Omega; L^\infty((0, T)))$  and if the initial values contain a jump no more regularity can be expected. Thus, the test functions have to be differentiable,  $V = H^1(\Omega; H^1(0, T))$ , such that the weak form has a meaning. On the other hand, the solution of the dual problem, which is again an advection equation, will only be in  $L^\infty(\Omega; L^\infty(T, 0))$  and consequently not necessarily in  $V$ . Consequently, the adjoint solution  $z$  need not be regular enough to be used as a test function in (1). See also [21, Example B] for a more detailed exposition.

There are two obvious possibilities to match the solution spaces and test spaces in this setting: For a linear problem, modification of the goal functional, and consequently the data of the dual problem, can increase the regularity of the dual solution  $z$  and allow  $z$  to be used as a test function in (1). Second, and more generally applicable to nonlinear problems, artificial viscosity can be used to prevent shocks and obtain sufficiently smooth adjoint solutions, see for instance [19]. The method presented subsequently in the paper at hand can do without modification in the primal equation and only relies on artificial viscosity in the dual equation.

The problem of non-fitting solution and test spaces for the primal and dual problem is also mentioned in [5, Remark 2.3].

### 3 Discontinuous test case (1 dimensional)

In this section, the solutions of a 1D advection problem and a 1D advection diffusion problem with discontinuous initial data are computed analytically. Additionally, for both cases an adjoint problem with discontinuous initial data is given and the analytic solutions are determined. The four solutions, two primal and two dual, are used to compute weighted residuals which are needed for the DWR method.

It is shown, that the weighted residual for the advection equation with weight given by the adjoint solution for advection diffusion equation, do not

converge for vanishing viscosity in the adjoint problem. This shows the capriciousness of evaluating the weighted residual of the advection equation with the formal dual given by (2).

### 3.1 The pure advection equation and its dual

A simple advection problem for  $x \in \mathbb{R}$  and  $t \in (0, T)$  is given by

$$\partial_t u_0(x, t) + \partial_x u_0(x, t) = 0, \quad \text{in } \mathbb{R} \times (0, T), \quad (3)$$

with initial condition

$$u_0(x, 0) = u_{ini}(x) = \begin{cases} 1, & -1 \leq x \leq 0, \\ 0, & \text{else.} \end{cases} \quad (4)$$

Since the advection diffusion equation is introduced later in this paper, the solution of the advection equation is marked as  $u_0$ , which is compatible with zero diffusion. With the discontinuous initial condition the problem is only reasonable in weak sense: For all  $\psi \in C_c^1(\mathbb{R} \times [0, T])$ , differentiable test functions with compact support in  $\mathbb{R}$ , it holds

$$a_0(u_0, \psi) := - \int_0^T \int_{\mathbb{R}} u_0 \partial_t \psi + u_0 \partial_x \psi \, dx \, dt + \int_{\mathbb{R}} (u_{ini}(x) - u_0(x, 0)) \psi(x, 0) \, dx = 0. \quad (5)$$

The weak solution for  $t \leq T$  is given by

$$u_0(x, t) = u_{ini}(x - t) = \begin{cases} 1, & -1 + t \leq x \leq t, \\ 0, & \text{else} \end{cases} \quad (6)$$

which is simply a translation of the initial condition along the characteristic curves.

Choosing the goal functional as

$$J(u_0) = \int_{\mathbb{R}} u_0(x, T) z_T(x) \, dx, \quad (7)$$

with the weight  $z_T$  indicating an area of interest

$$z_T(x) := \begin{cases} 1, & 0 \leq x \leq 1, \\ 0, & \text{else} \end{cases}$$

gives a dual problem of the above advection equation, an advection equation backwards in time with discontinuous initial data. This dual problem can be formulated in the weak sense as: For all  $\psi \in C_c^1(\mathbb{R} \times (0, T])$  :

$$\int_0^T \int_{\mathbb{R}} z_0 \partial_t \psi + z_0 \partial_x \psi \, dx \, dt - \int_{\mathbb{R}} (z_T(x) - z_0(x, T)) \psi(x, T) \, dx = 0,$$

with initial condition  $z_0(x, T) = z_T(x)$ .

Fixing  $T = 1$ , the solution for  $t \in (0, 1)$  is

$$z_0(x, t) = \begin{cases} 1, & -1 + t \leq x \leq t, \\ 0, & \text{else,} \end{cases}$$

which coincides with the primal solution.

As we have seen above, the advection equation and its adjoint provide solutions in  $L^\infty(\mathbb{R}; L^2(0, 1))$ . To obtain solutions in  $H^1(\mathbb{R}; H^1(0, 1))$  the advection problem can be modified with a small diffusion, as done in the vanishing viscosity method, e.g., [10, pp 403]. Notice, that in [10] the initial condition is in  $H^1(\mathbb{R})$  and the solution therefore of higher regularity than in the case considered below. In the following, the advection diffusion equation is initialized with the same step function as before, which is only  $L^\infty(\mathbb{R})$ . The solution is calculated analytically and examined regarding its regularity.

### 3.2 The advection diffusion equation and its dual

The one dimensional advection diffusion equation with diffusion coefficient  $\varepsilon > 0$  reads

$$\partial_t u_\varepsilon(x, t) + \partial_x u_\varepsilon(x, t) - \varepsilon \partial_{xx} u_\varepsilon(x, t) = 0 \quad (8)$$

in the domain  $\mathbb{R} \times (0, 1)$ . Again, the following initial condition (4) is assumed.

The weak solution  $u_\varepsilon$  of the advection diffusion equation satisfies

$$\begin{aligned} a_\varepsilon(u_\varepsilon, \psi) &= - \int_0^1 \int_{\mathbb{R}} u_\varepsilon \partial_t \psi + u_\varepsilon \partial_x \psi - \varepsilon \partial_x u_\varepsilon \partial_x \psi \, dx \, dt \\ &\quad + \int_{\mathbb{R}} (u_{\text{ini}}(x) - u_0(x, 0)) \psi(x, 0) \, dx \\ &= 0, \end{aligned} \quad (9)$$

for all  $\psi \in H_c^1(\mathbb{R}; H^1(0, 1))$ . The known Green's function for this problem (see [28, pp. 9–12]) is

$$G(x, \xi, t) = \frac{1}{\sqrt{4\pi t \varepsilon}} e^{-\frac{(x-\xi-t)^2}{4t\varepsilon}}$$

for  $\xi \in \mathbb{R}$ . Thus, the solution  $u_\varepsilon$  is given by

$$u_\varepsilon(x, t) = \frac{1}{\sqrt{\pi}} \int_{\frac{x-t}{2\sqrt{t\varepsilon}}}^{\frac{x+1-t}{2\sqrt{t\varepsilon}}} e^{-y^2} \, dy,$$

where the integral and its factor  $\frac{1}{\sqrt{\pi}}$  can be expressed in terms of the error function (see [13, Definition 3.1.1]), providing the alternative representation

$$u_\varepsilon(x, t) = \frac{1}{2} \left( \operatorname{erf} \left( \frac{x + 1 - t}{2\sqrt{t\varepsilon}} \right) - \operatorname{erf} \left( \frac{x - t}{2\sqrt{t\varepsilon}} \right) \right). \quad (10)$$

This solution corresponds to the one provided in the test case 'Advection and diffusion of a plane wave in a channel' in [6].

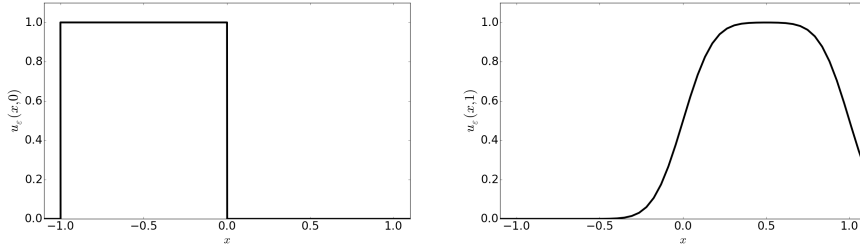


**Fig. 1** Initial condition  $u_\varepsilon(x, 0)$  (left) and solution  $u_\varepsilon(x, 1)$  (right).

Figure 1 shows the initial step function and the solution at  $t = 1$  which propagates to the right. Furthermore, one can see the smoothening caused by diffusion with diffusion parameter  $\varepsilon = 0.01$ . Having the primal solution, the adjoint solution is to be computed next.

The adjoint equation to the one dimensional advection diffusion equation, with respect to the same goal functional (7) as in the advection case, is

$$-\partial_t z_\varepsilon(x, t) - \partial_x z_\varepsilon(x, t) - \varepsilon \partial_{xx} z_\varepsilon(x, t) = 0 \quad \text{in } \mathbb{R} \times (1, 0) \quad (11)$$

with the initial conditions  $z_\varepsilon(x, 1) = z_T(x)$ . In analogy to the primal case the solution of the dual problem is given by

$$z_\varepsilon(x, t) = \frac{1}{2} \left( \operatorname{erf} \left( \frac{-x + 1 - (1 - t)}{2\sqrt{(1 - t)\varepsilon}} \right) - \operatorname{erf} \left( \frac{-x - (1 - t)}{2\sqrt{(1 - t)\varepsilon}} \right) \right), \quad (12)$$

using the transformation  $(x, t) \rightarrow (-x, 1 - t)$ . Here the dual solution  $z_\varepsilon$  is in  $H_{\text{loc}}^1(\mathbb{R}; H^1((0, 1)))$  and therefore the weak derivative necessary for the residual can be applied to  $z_\varepsilon$ .

### 3.3 Pure advection residual

Application of the DWR method to the purely advective case needs the evaluation of  $a_0(\cdot, \cdot)$  at  $(u_0, z_0 - z_0^{hk})$ , compare equation (5), where  $z_0^{hk}$  is the solution of the time and space discretized advection equation. In the example at hand, the solution  $z_0$  is in  $L^\infty(\mathbb{R}; L^2(0, 1))$ , as is  $z_0 - z_0^{hk}$ . To evaluate (5), time and space derivatives of  $z_0 - z_0^{hk}$  have to be considered. This could be done in

the distributional sense, but only if the function to which the distribution is applied to is in  $H^1(\mathbb{R}; H^1(0, 1))$ . This is not the case for  $u_0 \in L^\infty(\mathbb{R}; L^2(0, 1))$  which does not have a weak derivative. The nonexistence of derivatives of the primal and dual solution at the same point is due to coinciding discontinuities of the solutions.

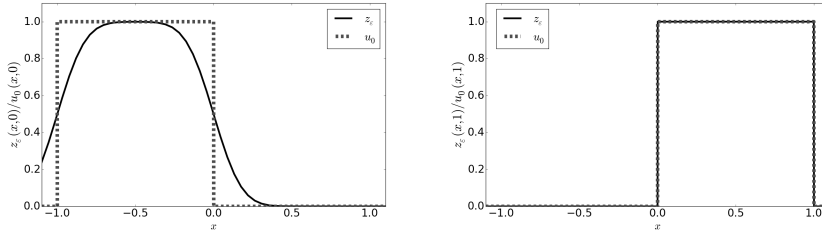


**Fig. 2** Artificial viscosity (here  $\varepsilon = 0.01$ ) in the dual asserts that coinciding discontinuities appear only at  $t = 1$  (right) and not at  $t = 0$  (left).

To avoid coinciding discontinuities at  $t = T$ , the dual initial condition would have to be modified but this can only be done by modification of the goal functional which is not in the interest of applications. Thus, for the weighted residuals in Section 4, the solution of the dual advection diffusion equation is taken, since this solution is differentiable on  $\Omega \times (0, T)$ .

More general, it is necessary that one solution - primal or dual - is sufficiently smooth, the weighted residual can be computed and thus be used for error estimation in the DWR method. This suggests to force one solution to be smooth with a modification in the equation, an artificial viscosity. Since the interest lies in the primal solution it is reasonable to modify the dual equation and thus obtain a slightly different, smoother dual solution. In doing this, the question of the thereby introduced error arises. Therefore, in the next section, the DWR error estimator for a modified dual equation is determined.

#### 4 Error estimator with correction term

In this section, an additional term in the goal oriented error estimator is identified, which is caused by a modification of the dual equation. The primal equation is considered with a source term as

$$a_0(u_0, \psi) = S(\psi) =: \int_0^1 \int_{\mathbb{R}} f \psi \, dx \, dt \quad \forall \psi \in V. \quad (13)$$

Following [5], the Lagrangian is set to

$$L(u_0, z_0) := J(u_0) + S(z_0) - a_0(u_0, z_0). \quad (14)$$

The formal dual problem is obtained as a stationary point of the Lagrangian, and gives the known problem

$$a'_0(u_0; \phi, z_0) = J'(u_0; \phi) \quad \forall \phi \in V. \quad (15)$$

As we have seen above, this dual problem might return a  $z_0$  which is not in the intersection  $V \cap W$ , and thus  $z_0$  might not be an admissible function in the test function space of the primal equation, (13). For this reason, we add artificial viscosity to the dual problem and the new dual equation with the smooth dual solution  $z_\varepsilon \in V$  reads

$$a'_\varepsilon(u_0; \phi, z_\varepsilon) = J'(u_0; \phi) \quad \forall \phi \in V$$

and it holds pointwise almost everywhere  $\lim_{\varepsilon \rightarrow 0} z_\varepsilon = z_0$ . With this, the difference between the value of the goal functional of the exact solution  $u_0$  and the value of the goal functional of the numerically approximated solution  $u^{hk}$ , can be represented as the difference of the Lagrangian of the exact solution and of the discrete one. The commonly applied test function is the -usually smooth- dual solution  $z_0$  because it makes an additional residual vanish, compare [5]. But here the solution of the modified dual equation,  $z_\varepsilon$ , needs to be used. In the following, the influence of this change shall be determined. For this, the Lagrangian has to be differentiated. Let  $L'(u_0; u_0 - u_0^{hk}, z_\varepsilon)$  be the derivative with respect to the first variable in direction of  $u_0 - u_0^{hk}$ , and  $L'(u_0, z_\varepsilon; z_\varepsilon - z_\varepsilon^{hk})$  be the derivative with respect to the second variable in  $z_\varepsilon - z_\varepsilon^{hk}$  direction. Thus,

$$\begin{aligned} J(u_0) - J(u_0^{hk}) &= L(u_0, z_\varepsilon) - L(u_0^{hk}, z_\varepsilon^{hk}) \\ &= \frac{1}{2} L'(u_0; u_0 - u_0^{hk}, z_\varepsilon) + \frac{1}{2} L'(u_0^{hk}; u_0 - u_0^{hk}, z_\varepsilon^{hk}) \\ &\quad + \frac{1}{2} L'(u_0, z_\varepsilon; z_\varepsilon - z_\varepsilon^{hk}) + \frac{1}{2} L'(u_0^{hk}, z_\varepsilon^{hk}; z_\varepsilon - z_\varepsilon^{hk}) \\ &\quad + \tilde{R}, \end{aligned} \quad (16)$$

where the remainder term  $\tilde{R}$  is given in terms of the error  $e := (u_0, z_\varepsilon) - (u_0^{hk}, z_\varepsilon^{hk})$ , analogous to [5], as

$$\tilde{R} = \frac{1}{2} \int_0^1 L''((u_0^{hk}, z_\varepsilon^{hk}) + se; e, e) ds = 0.$$

Here the remainder is zero, since the Lagrangian is linear in this example. The definition of the Lagrangian, (14), is plugged into expansion of the Lagrangian (16) and the difference in the goal functional reads

$$\begin{aligned} J(u_0) - J(u_0^{hk}) &= \frac{1}{2} \left[ \rho^*(z_\varepsilon^{hk}, u_0 - u_0^{hk}) + \rho(u_0^{hk}, z_\varepsilon - z_\varepsilon^{hk}) \right. \\ &\quad \left. + \rho^*(z_\varepsilon, u_0 - u_0^{hk}) + \rho(u_0, z_\varepsilon - z_\varepsilon^{hk}) \right] \end{aligned}$$

with the primal and dual residuals

$$\rho(u_0, z_\varepsilon - z_\varepsilon^{hk}) := S(z_\varepsilon - z_\varepsilon^{hk}) - a_0(u_0, z_\varepsilon - z_\varepsilon^{hk}) = 0, \quad (17)$$

$$\rho^*(z_\varepsilon, u_0 - u_0^{hk}) := J'(u_0; u_0 - u_0^{hk}) - a'_0(u_0; u_0 - u_0^{hk}, z_\varepsilon). \quad (18)$$

Since,  $u_0$  solves equation (13) the the primal residual in  $u_0$  vanishes. Normally the weighted dual residual of the analytic dual solution vanishes. But for  $z_\varepsilon$  it does not. Thus, the error in the goal functional is given as

$$J(u_0) - J(u_0^{hk}) = \frac{1}{2} \left[ \rho^*(z_\varepsilon^{hk}, u_0 - u_0^{hk}) + \rho(u_0^{hk}, z_\varepsilon - z_\varepsilon^{hk}) + \rho^*(z_\varepsilon, u_0 - u_0^{hk}) \right]. \quad (19)$$

In comparison to the error given in [5] the first two residuals now contain  $z_\varepsilon$  instead of  $z_0$ , as was expected, but an additional dual residual,  $\rho^*(z_\varepsilon, u_0 - u_0^{hk})$  has to be taken into account.

Concluding, in this section it was shown that a modification in the dual equation introduces an additional dual residual. Given the goal functional of the above mentioned advection problem the error in the goal functional can be computed easily. This representation of the error in the goal functional which is due to the introduction of diffusion in the dual equation is going to be evaluated numerically in the next section.

## 5 Discretization schemes

Advection can develop or maintain discontinuities in the solutions, as seen in the advection example in Section 3. One approach for an accurate and efficient method to solve advection dominated problems numerically are the discontinuous Galerkin (DG) methods. These methods combined with slope limiters are able to capture the physically relevant discontinuities without producing spurious oscillations, [7].

Some of the first to apply the DG method were W. Reed and T. Hill, [17], in 1973. DG methods are generalizations of finite volume methods but possess also properties of finite element methods, as for instance the simple handling of complex geometries and of boundary conditions. The advantage of DG lies in the discontinuities at the element boundaries and the thereby resulting simple routines for parallelization and adaptivity. These advantages, however, have to be bought by the price of a higher number of degrees of freedom than for the continuous finite element schemes.

In this section, the primal advection equation and the dual diffusion equation from the examples above shall be spatially discretized in DG fashion to compute the dual weighted residual as necessary for the error estimation in the goal functional, see equation (19). Usually the weight in the residuals is approximated by a global higher order approximation, a patchwise higher order interpolation, or a cellwise interpolation estimate, [5], since the analytic solution is not given.

In the case at hand, the analytic solutions are known and thus an approximation is not necessary, which will be useful to demonstrate the advantage of our modified dual.

For the discretization the interval  $\Omega = [a, b]$  is decomposed into a set  $\mathcal{E}$  of  $n$  non-overlapping elements  $E$  of length  $h$  such that

$$\Omega = \bigcup_{E \in \mathcal{E}} E.$$

For each element  $E \in \mathcal{E}$  the flux in the element is defined as

$$F(u_\varepsilon)(x, t) := u_\varepsilon(x, t) - \varepsilon \partial_x u_\varepsilon(x, t), \quad (x, t) \in E \times (0, 1)$$

and thus for each  $E$  the weak form of the advection diffusion equation with no source term can be represented as

$$\begin{aligned} 0 = a_\varepsilon(u_\varepsilon, \psi) &= \sum_{E \in \mathcal{E}} \left\{ \int_0^1 \int_E \partial_t u_\varepsilon \psi + \partial_x F(u_\varepsilon) \psi \, dx \, dt + \int_E u_{ini}(x) \psi(x, 0) \, dx \right\} \\ &= \sum_{E \in \mathcal{E}} \left\{ \int_0^1 \int_E \partial_t u_\varepsilon \psi - F(u_\varepsilon) \partial_x \psi \, dx \, dt + \int_E u_{ini}(x) \psi(x, 0) \, dx \right. \\ &\quad \left. + \int_0^1 F(u_\varepsilon) \psi|_{\partial E} \, dt \right\}. \end{aligned}$$

Evaluation on the boundaries of the elements  $E$  is not straightforward, since a discontinuous Galerkin method allows jumps on the boundaries and thus the function value is not unique. In the application of DG methods, it is common, compare [7], to approximate the flux over the edge by a numerical flux  $F^*$ . For the computation of these boundary terms, the symmetric interior penalty Galerkin (SIPG) method, [27], is applied to the problem in this paper. This gives the boundary fluxes

$$\begin{aligned} \sum_{E \in \mathcal{E}} \int_0^1 F^*(u_\varepsilon) \psi|_{\partial E} \, dt &:= \sum_{\partial E \in \partial \mathcal{E}} \left\{ \int_0^1 \frac{N^2}{h} [u_\varepsilon][\psi] - \{\varepsilon \partial_x \psi\} [u_\varepsilon] - \{\varepsilon \partial_x u_\varepsilon\} [\psi] \, dt \right. \\ &\quad \left. + \int_0^1 u_{\varepsilon, l_E} \psi|_{l_E} \, dt \right\} \\ &+ \int_0^1 \left( \frac{N^2}{h} \psi(a, t) + \varepsilon \partial_x \psi_\varepsilon(a, t) \right) u_{\varepsilon, \text{bound}}(a, t) \, dt \\ &+ \int_0^1 \left( \frac{N^2}{h} \psi(b, t) - \varepsilon \partial_x \psi_\varepsilon(b, t) \right) u_{\varepsilon, \text{bound}}(b, t) \, dt \end{aligned}$$

$[\cdot]$  is the jump at the element edges,  $\{\cdot\}$  is the average of two element values at one edge, and  $u_{\varepsilon,l_E}$  is the evaluation of the left element on an element edge to obtain an upwind flux for the advection. Furthermore, Dirichlet boundaries on  $[a, b]$  are assumed and to mimic these values the boundary values  $u_{\varepsilon,\text{bound}}(\cdot, t)$  are computed as values of the analytic solution.

Choosing the test functions  $\psi^h$  in the finite dimensional space  $V^h = \{\psi \in L^2(\Omega) : \forall E \quad \psi|_E \in P_p(E)\}$  where  $P_p(E)$  is the space of polynomials of degree  $p$  on element  $E$  and the ansatz functions  $\psi_i|_E$  such that they construct a basis of  $V^h$ . The test function - the ansatz function respectively - can be represented as

$$\begin{aligned}\psi^h(x) &= \sum_{i=0}^p \psi_i(x), \\ u_\varepsilon^h(x, t) &= \sum_{i=0}^p u_{\varepsilon,i}(t) \psi_i(x).\end{aligned}$$

With these representations the semi discrete form on each element  $E$  is obtained:

$$0 = \partial_t u_{\varepsilon,i} \int_E \psi_i \psi_j \, dx - F(u_\varepsilon) \int_E \partial_x \psi_i \psi_j \, dx + F^*(u_{\varepsilon,i}) \psi_i \psi_j|_{\partial E}.$$

With the definition of element-wise matrices

$$M_{E,i,j} := \int_E \psi_i \psi_j \, dx, \quad D_{E,i,j} := \int_E \partial_x \psi_i \psi_j \, dx, \quad B_{E,i,j} := \psi_i \psi_j|_{\partial E},$$

it is

$$M_{E,i,j} \partial_t u_{\varepsilon,i} = -D_{E,i,j} F(u_{\varepsilon,i}) - B_{E,i,j} F^*(u_{\varepsilon,i}).$$

Inverting the mass matrix  $M_E = (M_{E,i,j})_{i,j}$  gives a semi discrete form

$$\partial_t u_\varepsilon = -M_E^{-1} D_E F(u_\varepsilon) - M_E^{-1} B_E F^*(u_\varepsilon),$$

which can be treated with time discretization schemes.

The primal advection equation is treated in a similar way, but the numerical flux is only the up-winding term  $F^*(u_0) = u_0^l$ .

In the example at hand, the explicit Euler method is used for time discretization and Lagrange Polynomials of degree two are used for spatial discretization by the above introduced DG method without any limiter. Though the explicit time discretization requires a step size restriction by the CFL condition, it is chosen to have an explicit representation of the discrete time derivative which is of value in the computation of the residuals. The time step size for the solution, plotted in Figure 3 and Figure 4, is  $k = 0.001$  and the spatial discretization uses elements of the size  $h = 0.125$ . With the DG method the box-shaped initial condition for the primal and the dual case can be initialized without any initialization error. For the purely advective primal

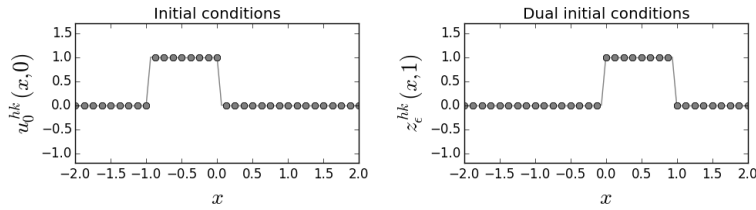


**Fig. 3** Initial condition of the primal and the dual problem

case, the box is advected to the right hand side with the unit velocity. The numerical advection causes some over and under shootings in front of steep gradients since no limiter is applied. The dual problem with diffusion advects the box to the left hand side and smooths the step gradients. In this case, the numerical solution is close to the analytical one.

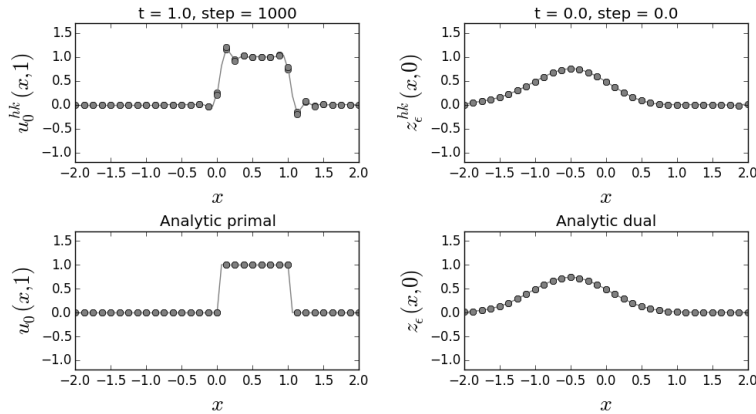


**Fig. 4** Solution of the primal (left) and the dual problem (right) at  $t = 1$  and  $t = 0$ , respectively, with  $k = 0.001$ ,  $h = 0.125$ , and dual diffusion coefficient  $\varepsilon = 0.1$  (first line). The second line shows the corresponding values of the known solution.

The dual initial condition is set at  $t = T$  and the simulation runs down to  $t = 0$  with a diffusion coefficient  $\varepsilon = 0.1$ . For sufficiently smooth solutions the SIPG method provides convergence of  $L^2$ -errors of the order  $p + 1$ , where  $p$  is the order of the polynomial, compare [18]. For discontinuous initial conditions, the order of convergence is lower.

In the numerical example at hand, the global  $L^2$ -error at final time  $T = 1$  of the primal solution of the advection equation (black dots) decreases proportional to  $\sqrt{h}$ , marked with a dashed line, as seen in Figure 5.

The right hand side of Figure 5 shows the decreasing global  $L^2$ -error of the dual problem of the advection diffusion equation. In this case, the error tends to a convergence rate of 1 (dashed line).

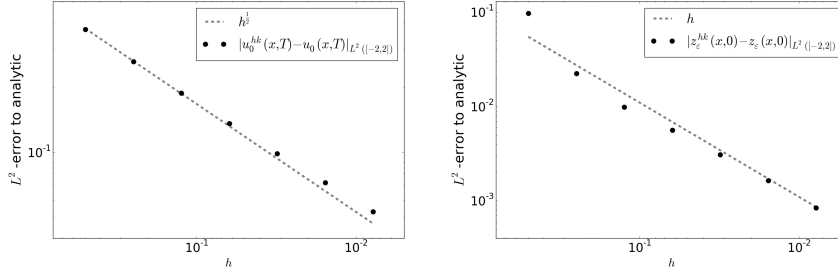


**Fig. 5** Global  $L^2$ -error of the (primal) advection problem at final time  $t = 1$  (left) and dual advection diffusion problem at final time  $t = 0$  (right) with  $\varepsilon = 0.1$ . The timestep in both cases is  $k = 0.001$ .

With the discrete solution of the dual advection diffusion equation and the discrete solution of the primal advection equation the weighted residuals, necessary for the error estimation in the goal functional, can be computed.

For the error estimation, the residuals are integrated by parts, such that the derivatives are applied to  $u_0^{hk}$ , for the primal problem, and  $z_\varepsilon^{hk}$ , for the dual problem, respectively. The integrals are computed by quadrature formulas on each of the elements/time intervals that are combined for the global space time integral. If  $M + 1$  quadrature points per element are used in space and a total of  $N + 1$  quadrature points in time the discrete, global in time, element-wise residual is evaluated as:

$$\begin{aligned}
\rho_E^{hk}(u_0^{hk}, z_\varepsilon - z_\varepsilon^{hk}) &:= \sum_{i=0}^M \sum_{j=0}^N w_i \tilde{w}_j u_0^{hk}(x_i, t_j) \\
&\quad \left( (z_\varepsilon - z_\varepsilon^{hk})(x_i, t_{j+1}) - (z_\varepsilon - z_\varepsilon^{hk})(x_i, t_j) \right) \\
&\quad - k \sum_{i=0}^M \sum_{j=0}^N w_i \tilde{w}_j \partial_x u_0^{hk}(x_i, t_j) (z_\varepsilon - z_\varepsilon^{hk})(x_i, t_j) \\
&\quad + k \sum_{j=0}^N \tilde{w}_j u_0^{hk}(x_{E,\text{right}}, t_j) (z_\varepsilon - z_\varepsilon^{hk})(x_{E,\text{right}}, t_j) \\
&\quad - k \sum_{j=0}^N \tilde{w}_j u_0^{hk}(x_{E,\text{left}}, t_j) (z_\varepsilon - z_\varepsilon^{hk})(x_{E,\text{left}}, t_j) \\
&\quad - \sum_{i=0}^M w_i u_0^{hk}(x_i, 1) (z_\varepsilon - z_\varepsilon^{hk})(x_i, 1),
\end{aligned} \tag{20}$$

where  $w_i$  are the element-wise quadrature weights in space and  $\tilde{w}_i$  are the weights in time. The discrete residual, equation (20), serves as element-wise error estimator

$$\eta_E^{hk} := \frac{1}{2} \rho_E^{hk}(u_0^{hk}, z_\varepsilon - z_\varepsilon^{hk}).$$

The dual residual is treated analogously:

$$\begin{aligned}
\rho_E^{*hk}(z_\varepsilon, u_0 - u_0^{hk}) &= - \sum_{i=0}^M w_i (u_0 - u_0^{hk})(x_i, 1) z_\varepsilon(x_i, 1) \\
&+ k \sum_{i=0}^M \sum_{j=0}^N w_i \tilde{w}_j u_0(x_i, t_j) \partial_x z_\varepsilon(x_i, t_j) \\
&+ k \sum_{i=0}^M \sum_{j=0}^N w_i \tilde{w}_j \partial_x u_0^{hk}(x_i, t_j) z_\varepsilon(x_i, t_j) \\
&+ \sum_{i=0}^M \sum_{j=0}^N w_i \tilde{w}_j (u_0 - u_0^{hk})(x_i, t_j) \\
&\quad (z_\varepsilon(x_i, t_{j+1}) - z_\varepsilon(x_i, t_j)) \\
&+ k \sum_{j=0}^N \tilde{w}_j u_0^{hk}(x_{E,\text{right}}, t_j) z_\varepsilon(x_{E,\text{right}}, t_j) \\
&- k \sum_{j=0}^N \tilde{w}_j u_0^{hk}(x_{E,\text{left}}, t_j) z_\varepsilon(x_{E,\text{left}}, t_j)
\end{aligned} \tag{21}$$

and the same for  $\rho_E^{*hk}(z_\varepsilon^{hk}, u_0 - u_0^{hk})$ . The sum of the dual residuals is set to be the element-wise dual error estimator

$$\eta_E^{*hk} := \frac{1}{2} \rho_E^{*hk}(z_\varepsilon, u_0 - u_0^{hk}) + \frac{1}{2} \rho_E^{*hk}(z_\varepsilon^{hk}, u_0 - u_0^{hk}).$$

Since we are interested in the quality of the global error estimate, we refrain from a separation of the indicators into a separate space and time contribution.

Following equation (19), the element-wise evaluated discrete primal and dual weighted residuals define a local error estimator

$$\eta_E := \eta_E^{hk} + \eta_E^{*hk} \tag{22}$$

and the sum over all elements is an approximation of the global error

$$\eta^{hk} := \sum_{E \in \mathcal{E}} \eta_E \approx J(u_0) - J(u_0^{hk}). \tag{23}$$

We remark, that although all terms in the residuals are known, due to the integration error only an approximation of the residuals is computed. Since we will consider the limit  $\varepsilon \rightarrow 0$  this quadrature error needs to be kept in mind.

## 6 Numerical experiments

In this section, the dependence of the absolute value of the additional residual on the spatial grid size is studied numerically. Then, the behavior of the local error estimators with and without the additional dual residual is further investigated, and, in the end, the global error estimator including the additional residual is found to gain a better effectivity index as the global estimator without the artificial viscosity.

In the following the spatial discretization on  $\Omega = [-2, 2]$  in DG manner uses basis and test function polynomials of order 2 and the discrete solutions are evaluated such that a numerical quadrature, using a summarized trapezoidal rule on each element, can be performed. An example shows the influence of the choice of the quadrature rule. The value of the goal functional for the discrete solution,  $J(u_0^{hk})$ , is also determined exactly by the trapezoidal rule. The goal value of the analytic solution,  $J(u_0)$ , is one.

In this setting, the global value of the additional residual was computed for different spatial resolutions and a fixed time step size of  $k = 0.0001$ .

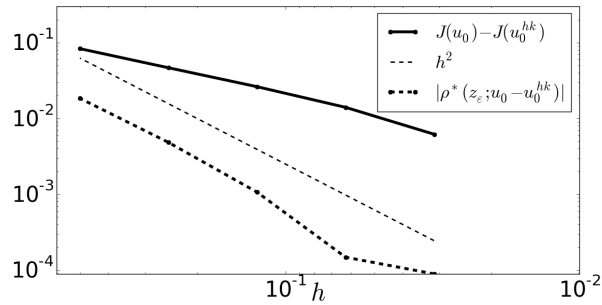


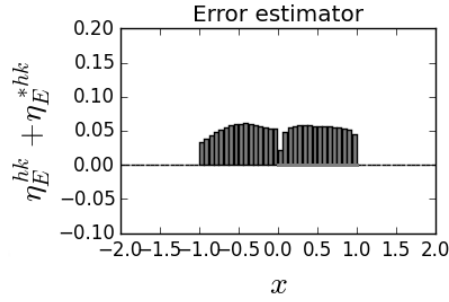
Fig. 6 Absolute value of the additional residual,  $k = 0.0001$ ,  $\varepsilon = 0.1$ .

Figure 6 shows the absolute global value of the additional residual for  $\varepsilon = 0.1$ . This extra term converges with second order to zero and is thus faster than the actual error in the goal functional, implying the finer the mesh, the less important the additional residual.

However, the difference to the classical formulation is not only the additional residual, but also the replacement of the discontinuous dual function by the solution of the dual advection diffusion equation.

All three residuals together, element-wise evaluated, give the local error estimators, see (22). For a uniform grid the local error estimator  $\eta_{E,uni}$  indicates the area of influence for the goal functional, (7).

The area of interest, on which the goal functional is evaluated, is the interval  $[0, 1]$ . Thus, for the discontinuous test case presented in this paper, each element over which the box shaped function moves, has theoretically an equally high local error estimator, while the regions outside are of minor influence to



**Fig. 7** Absolute value of local error estimators on a uniform grid with  $h = 0.0625$  and artificial viscosity  $\varepsilon = 0.05$

the value of the goal functional. This is reflected in the numerical results, as, e.g., in Figure 7, despite the diffusion in the dual the estimator does not smear.

Dörfler marking, [8], would suggest to refine the elements in the middle of Figure 7, namely in the interval  $I_{\text{ref}} = [-1, 1]$ , such that the  $l_2$  norm of the estimator in the set which is going to be refined,  $\mathcal{E}_{\text{ref}}$ , is larger than a specific percentage of the  $l_2$  norm of the estimators in the whole set  $\mathcal{E}$ ,

$$\sqrt{\sum_{E \in \mathcal{E}_{\text{ref}}} (\eta_E^{hk} + \eta_E^{*hk})^2} \geq (1 - \Theta) \sqrt{\sum_{E \in \mathcal{E}} (\eta_E^{hk} + \eta_E^{*hk})^2},$$

for some  $\Theta \in (0, 1)$ . In the test case at hand, refinement in  $I_{\text{ref}}$  is achieved with  $1 - \Theta \approx 1 - 10^{-6}$ , showing that most of the estimated error is in  $I_{\text{ref}}$ .

The summation over each element of the signed local spatial error estimators on the uniform grid brings the global estimator  $\eta_{\text{uni}}^{hk}$ , while the sum of the estimators over the locally refined, grid brings  $\eta_{\text{ref}}^{hk}$ .

**Table 1** Dependence of the global error estimators and the error in the goal functional on the grid size. Uniform grid size  $h$  is marked in bold.  $\varepsilon = 0.1$

$h$	$\eta_{\text{uni}}^{hk}$	$\eta_{\text{ref}}^{hk}$	$ J(u_0) - J(u_{0,\text{uni}}^{hk}) $	$ J(u_0) - J(u_{0,\text{ref}}^{hk}) $
<b>0.5</b> /0.25	0.0674	0.0552	0.0832	0.0466
<b>0.25</b> /0.125	0.0437	0.0324	0.0466	0.0262
<b>0.125</b> /0.0625	0.0258	0.0174	0.0262	0.0140
<b>0.0625</b> /0.03125	0.0140	0.0080	0.0140	0.0062

Table 1 shows that the global error estimator on a uniform grid is greater than the estimator on a mesh which is locally refined once by bisection according to the error indicators. The bold  $h$  indicates the uniform grid size, the normal style  $h$  is the size of the refined elements. Also the error in the goal functional evaluated on a locally refined grid is smaller than on the uniform grid. On each element, the quadrature rule is the same, such that the

approximation of the integral is better in the refined elements. But the numerically evaluated error estimator does not satisfy the error identity, as suggested in equation (19). This could be caused by several reasons, for instance by a quadrature error or by a non-adjoint consistent implementation [12]. However, as the difference between estimator and error decrease with decreasing element size  $h$ , we do not investigate this issue further.

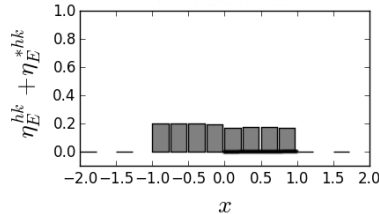


**Fig. 8** Absolute value of local error estimators on a locally refined grid with  $h = 0.5, 0.25$ , and  $\varepsilon = 0$

If the dual equation is not modified and the computations are done nevertheless by evaluating only

$$\eta_{E0} := \rho_E^{hk}(u_0^{hk}, z_0 - z_0^{hk}) + \rho_E^{*hk}(z_0^{hk}, u_0 - u_0^{hk}), \quad (24)$$

compare equation (22), the local error estimators are even more evenly distributed on the area which is expected to be refined, as shown in Figure 8. For the computation it was naively assumed, that  $\partial_x z_0 = \partial_t z_0 = 0$  in  $[-2, 2]$ , since this is true almost everywhere – and in particular in the chosen quadrature points.

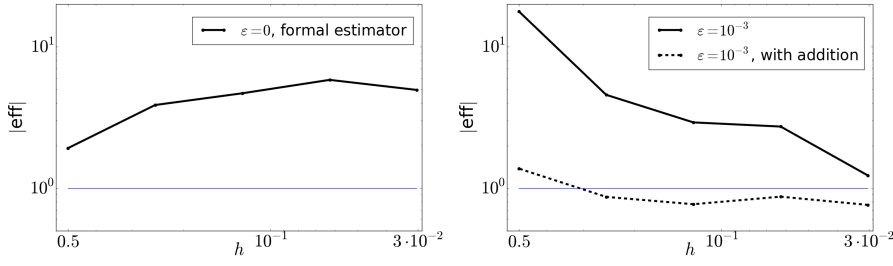
Concluding, the modification of the dual equation does not harm the local error indication, and even the approach without modification – ignoring the unboundedness in the analytic case – results in reasonable local error indication. So far, there seems to be no advantage in the modification, but this is different for the global error estimation:

The quality of the global error estimators is measured by the effectivity index, see, e.g., [25], [3], and [2], which is the ratio of the estimator to the true error. Here it is

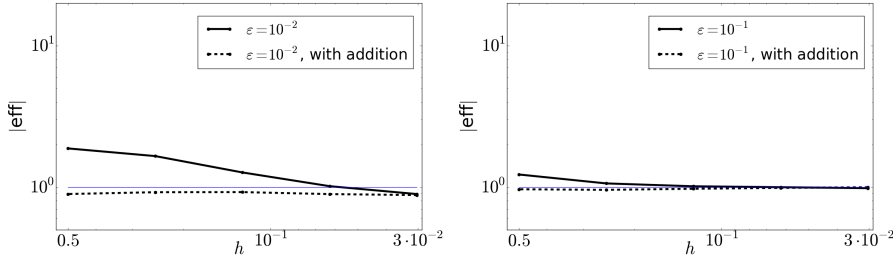
$$\text{eff} = \frac{J(u_0) - J(u_0^{hk})}{\eta^{hk}}.$$

Figure 9 shows the behavior of the effectivity index with respect to the spatial grid size. The index for the global error estimator without viscosity, e.g., equation (24), is increasing at first. If it ever converges to one, it is much later as in case of the modified error estimator.

The right hand side of Figure 9 shows that the error estimator including the additional residual gains a better effectivity on coarse grids as the estimator without the additional term, e.g. equation (23) with and without the last residual. Figure 10 depicts this relation also for different values of  $\varepsilon$ . For any



**Fig. 9** Effectivity of the global estimator without artificial viscosity in the dual equation (left) and with and without the additional residual,  $\rho^*(z_\varepsilon, u_0 - u_0^{hk})$  with viscosity  $\varepsilon = 0.001$  in the dual equation (right).



**Fig. 10** Effectivity of the global estimator with and without the additional residual,  $\rho^*(z_\varepsilon, u_0 - u_0^{hk})$ , for  $\varepsilon = 0.01$  (left) and  $\varepsilon = 0.1$  (right).

tested  $\varepsilon \in [0.0001, 0.1]$  the effectivity of the estimator including the addition was closer to one, but obviously depending on the diffusion coefficient. Thus, the relation of the error and the error estimator to the diffusion parameter  $\varepsilon$  is of interest. Table 2 shows the different global spatial error estimators for a decreasing diffusion coefficient. For stability reasons, the time step size was chosen to be  $k = 0.0001$  and the spatial grid size was fixed at  $h = 0.0625$ . Since neither the primal problem nor the goal functional are modified, the error in the goal functional is constant for a fixed grid size.

**Table 2** Dependence of the global spatial error estimators and on the dual diffusion coefficient  $\varepsilon$ , with  $J(u_0) - J(u_0^{hk}) = 0.0140$

$\varepsilon$	$ \eta_{\text{uni}}^{hk} $	$ \text{eff} $
0.0	0.0028	4.9515
0.0001	0.0076	1.8389
0.001	0.0051	2.7269
0.01	0.0138	1.0154
0.1	0.0140	0.9986

While the error in the goal functional is not influenced by the modification in the dual equation, the error estimator and thus the effectivity is. Notice, that for an exact evaluation of the residuals the effectivity is always one -

since an error identity is evaluated. However, with a fixed integration accuracy smaller values of  $\varepsilon$  increase the quadrature error and consequently effectivity deteriorates. Once the mesh is sufficiently refined the quadrature - fixed per element - gains accuracy and thus the effectivity converges to one. The same effect has to be expected when numerically recovering the unknown primal and dual solutions for the weights, as the accuracy of the discrete primal and dual solutions are fixed on a given mesh and can only be increased by refinement.

A ratio of the advection to the diffusion is given by the Peclet number, see, e.g., [14]. Here,  $P_h$  shall be the approximation of the Peclet number for a constant advection velocity of one, depending on the mesh size as  $P_h = \frac{h}{\varepsilon}$ .

**Table 3** Effectivity and approximated Peclet number for  $\varepsilon = 0.0001$  (left),  $\varepsilon = 0.01$  (middle), and  $\varepsilon = 0.1$  (right), with  $k = 10^{-4}$  constant and 40 quadrature points for a composite trapezoidal rule.

$h$	$\varepsilon = 0.0001$		$\varepsilon = 0.01$		$\varepsilon = 0.1$	
	$P_h$	eff	$P_h$	eff	$P_h$	eff
0.5	5000	-1.995	50	1.924	5	1.235
0.25	2500	-3.815	25	1.678	2.5	1.065
0.125	1250	7.290	12.5	1.277	1.25	1.016
0.0625	625	1.885	6.26	1.018	0.626	1.000

Table 3 shows that the effectivity of the global error estimator is getting better, the more the diffusion is of influence in the discretized scheme. Thus, it is suggested that, if the diffusion is resolved sufficiently, the modified dual weighted residual error estimator gives an effective approximation of the global error in the goal functional.

Concluding, these experiments suggest that in this setting the modified dual weighted residual error estimator for a spatial refinement is a reasonable indicator for grid refinement with respect to some goal functional and moreover the modified global error estimator is in this case of discontinuities a better approximation of the actual global error than the classical approach.

## 7 Summary and conclusion

The solutions of the advection equation and the advection diffusion equation, as well as their dual equations, all initialized with a step function, were recapitulated to provide necessary definitions for the problem setting. In case of coinciding discontinuities the convergence is a more subtle matter. If the adjoint of the discretized problem is used, the case of coinciding discontinuities does not appear since the discretized solution has bounded gradients. Thus, the order of discretization and optimization is of influence to the error estimator. To avoid these difficulties in the continuous problem setting, the dual equation was modified by a small artificial viscosity term and the solution of the modified dual does not exhibit discontinuities.

Due to the convergence of the residuals, the DWR error estimator changes only slightly if the dual of the advection equation is replaced with the dual of the advection diffusion equation. The advantage of the modification of the dual problem, instead of the primal one, is that the primal problem and the goal functional are unaffected by this change. For this modification, a modified dual weighted residual error estimator was derived as

$$J(u_0) - J(u_0^{hk}) = \frac{1}{2} \left[ \rho^*(z_\varepsilon^{hk}, u_0 - u_0^{hk}) + \rho(u_0^{hk}, z_\varepsilon - z_\varepsilon^{hk}) + \rho^*(z_\varepsilon, u_0 - u_0^{hk}) \right] + \tilde{R}.$$

This error estimator has an additional dual residual,  $\rho^*(z_\varepsilon, u_0 - u_0^{hk})$ , in comparison to the classical setting. Though the direct implementation without the modification showed similar absolute values for the local error estimators, the effectivity of the global error estimator without diffusion in the dual equation was, for the tested parameters, much larger than one and did not exhibit convergence towards one. The effectivity index of the modified problem, on the other hand, converged to one.

This leads to the conclusion that both approaches are applicable in practice if the focus is on error indication and local grid refinement. If the aim is to provide a good global error estimator, in terms of effectivity, the modified error estimator is to be preferred.

## References

1. M. Ainsworth and J. T. Oden. A posteriori error estimation in finite element analysis. *Computer methods in applied mechanics and engineering*, 142:1–88, 1997.
2. I. Babuška and W. C. Rheinboldt. A-posteriori error estimates for the finite element method. *International journal for numerical methods in engineering*, 12(10):1597–1615, 1978.
3. I. Babuška, R. Durán, and R. Rodríguez. Analysis of the efficiency of an a posteriori error estimator for linear triangular finite elements. *SIAM Journal on numerical analysis*, 29(4):pp. 947–964, 1992.
4. W. Bauer, M. Baumann, L. Scheck, A. Gassmann, V. Heuveline, and S. C. Jones. Simulation of tropical-cyclone-like vortices in shallow-water ICON-hex using goal-oriented r-adaptivity. *Theoretical and computational fluid dynamics*, 28(1):107–128, 2014.
5. R. Becker and R. Rannacher. An optimal control approach to a posteriori error estimation in finite element methods. *Acta numerica 2001*, 10:1–102, 2001.
6. D. Calhoun and R. J. LeVeque. A cartesian grid finite-volume method for the advection-diffusion equation in irregular geometries. *Journal of computational physics*, 157(1):143–180, 2000.
7. B. Cockburn, G. E. Karniadakis, and C. Shu. *The development of discontinuous Galerkin methods*. Springer, 2000.
8. W. Dörfler. A convergent adaptive algorithm for Poisson’s equation. *SIAM Journal on numerical analysis*, 33(3):1106–1124, June 1996.
9. K. Eriksson, D. Estep, P. Hansbo, and C. Johnson. Introduction to adaptive methods for differential equations. *Acta Numerica*, 4:105–158, 1995.
10. L. C. Evans. *Partial Differential Equations*. Graduate studies in mathematics. American Mathematical Society, 2010.

11. M. B. Giles and S. Ulbrich. Convergence of linearized and adjoint approximations for discontinuous solutions of conservation laws. part 1: Linearized approximations and linearized output functionals. *SIAM Journal on numerical analysis*, 48(3):882–904, 2010.
12. R. Hartmann. Adjoint consistency analysis of discontinuous Galerkin discretizations. *SIAM journal on numerical analysis*, 45(6):2671–2696, 2007.
13. E. W. Ng and M. Geller. A table of integrals of the error functions. *Journal of research of the national bureau of standards - B. Mathematical sciences*, 73B(1):3, 1969.
14. S. Patankar. *Numerical heat transfer and fluid flow*. CRC press, 1980.
15. P. W. Power, M. D. Piggott, F. Fang, G. J. Gorman, C. C. Pain, D. P. Marshall, A. J. H. Goddard, and I. M. Navon. Adjoint goal-based error norms for adaptive mesh ocean modelling. *Ocean modelling*, 15(1):3–38, 2006.
16. F. Rauser, P. Korn, and J. Marotzke. Predicting goal error evolution from near-initial-information: A learning algorithm. *Journal of computational physics*, 230(19):7284 – 7299, 2011.
17. W. H. Reed and T. R. Hill. Triangular mesh methods for the neutron transport equation. *Los Alamos Report LA-UR-73-479*, 1973.
18. B. Rivière. *Discontinuous Galerkin methods for solving elliptic and parabolic equations: Theory and implementation*. Society for Industrial and Applied Mathematics, 2008.
19. J. Schütz, G. May, and S. Noelle. Analytical and numerical investigation of the influence of artificial viscosity in discontinuous Galerkin methods on an adjoint-based error estimator. In *Computational fluid dynamics 2010*, pages 203–209. Springer, 2011.
20. T. Sonar and E. Süli. A dual graph-norm refinement indicator for finite volume approximations of the Euler equations. *Numerische Mathematik*, 78(4):619–658, 1998.
21. E. Süli and P. Houston. Adaptive finite element approximation of hyperbolic problems. In *Error estimation and adaptive discretization methods in computational fluid dynamics*, pages 269–344. Springer Berlin Heidelberg, 2003.
22. S. Ulbrich. A sensitivity and adjoint calculus for discontinuous solutions of hyperbolic conservation laws with source terms. *SIAM Journal on control and optimization*, 41(3):740–797, 2002.
23. S. Ulbrich. Adjoint-based derivative computations for the optimal control of discontinuous solutions of hyperbolic conservation laws. *Systems & control letters*, 48(3):313–328, 2003.
24. D. A. Venditti and D. L. Darmofal. Adjoint error estimation and grid adaptation for functional outputs: Application to quasi-one-dimensional flow. *Journal of computational physics*, 164(1):204–227, 2000.
25. R. Verfürth. A posteriori error estimation and adaptive mesh-refinement techniques. *Journal of computational and applied mathematics*, 50(1):67 – 83, 1994.
26. R. Verfürth. *A review of a posteriori error estimation and adaptive mesh-refinement techniques*. Wiley-Teubner, 1996.
27. M. F. Wheeler. An elliptic collocation-finite element method with interior penalties. *SIAM Journal of numerical analysis*, 15(1), 1978.
28. Z. Xu, J. R. Travis, and W. Breitung. *Green's function method and its application to verification of diffusion models of GASFLOW code*. Forschungszentrum Karlsruhe, 2007.